Available online at www.sciencedirect.com
SCIENCE DIRECT®
ELSEVIER
Bioorganic & Medicinal Chemistry 12 (2004) 529–535
Bioorganic & Medicinal Chemistry

The interaction of glycine, aspartic acid, and lysine by the protonated macrocyclic ligand 6,19-bis(2-hydroxypropyl)-3,6,9,16,19,22-hexaaza-tricyclo-[22.2.2.2^{11,14}]triaconta-11,13,24,26,27,29-hexaene☆

Jin Huang, Shu-An Li, Dong-Feng Li, De-Xi Yang, Wei-Yin Sun* and Wen-Xia Tang*

Coordination Chemistry Institute, State Key Laboratory of Coordination Chemistry, Nanjing University, Nanjing 210093, PR China

Received 28 May 2003; accepted 20 November 2003

Abstract—A new hexaaza macrocyclic ligand (L) bearing two 2-hydroxypropyl pendants, 6,19-bis(2-hydroxypropyl)-3,6,9,16,19,22-hexaaza-tricyclo-[22.2.2.2^{11,14}]triaconta-11,13,24,26,27,29-hexaene has been synthesized and characterized. The macrocyclic ligand was isolated as a colorless crystal, monoclinic, $P2(1)/n$, with $a = 10.757(2)$, $b = 14.214(3)$, $c = 13.746(3)$ Å, $\beta = 101.40(3)^\circ$, $V = 2060.3(7)$ Å^3, $Z = 2$, $R1 = 0.0695$, and w$R2 = 0.1538$ [$I > 2\sigma(I)$]. Potentiometric studies of the macrocyclic ligand and three types of amino acids, glycine (equal numbers of carboxylate and amino groups), aspartic acid (more carboxylate groups than amino group), and lysine (more amino groups than carboxylate group) have been performed. The stability constants for the new macrocycle and binary complexes of the amino acid with the macrocyclic ligand are reported. Binary complexes are formed in aqueous solution as a result of hydrogen bonding interaction and electrostatic attraction between the host and the guest. The binding Schemes for the recognition of amino acids are suggested. From the results, it seems that this new macrocyclic ligand is able to bind three different amino acids with selectivity in aqueous solution, and the strength of binding is of the order lysine < glycine < aspartic acid.

1. Introduction

The design and synthesis of new macrocyclic polyaza ligands are currently of great interest. The cavity, rigidity and donor type of a macrocycle are all important in governing the host–guest interactions.[1] In particular, the incorporation of functionalized pendant coordinating arms on macrocyclic polyaza compounds can provide additional coordinating functions and hence enchance the complexing stability. Some macrocycles with pendants have been reported previously. However, the synthesis of binucleating macrocyclic ligands with 2-hydroxypropyl pendants is rare. In this article, we report the structure of a new macrocyclic ligand, that is 6,19-bis(2-hydroxypropyl)-3,6,9,16,19,22-hexaaza-tricyclo-[22.2.2.2^{11,14}]triaconta-11,13,24,26,27,29-hexaene, $H_4L{\cdot}Br_2{\cdot}(ClO_4)_2{\cdot}2H_2O$.

The macrocyclic polyamines are capable of undergoing polyprotonation in solution, forming positively charged polyammonium cations which can selectively bind a variety of inorganic and organic substrates through hydrogen bonds and electrostatic forces.[2–9] The anions including phosphate, oxalate, malonate, pyrophosphate, and polyphosphate in aqueous solution bound to the polyazamacrocyclic ligands have been emphasized in recent years.[3–8] However, the interaction of amino acid molecules with macrocycles has rarely been investigated. The design of host molecules as receptors for the recognition of substrate anion guest in aqueous solution is a very important target from an environmental and health-related point of views with multiple potential applications.[10,11] Therefore, in the present work, the ability of 6,19-bis(2-hydroxypropyl)-3,6,9,16,19,22-hexaaza-tricyclo-[22.2.2.2^{11,14}]triaconta-11,13,24,26,27,29-hexaene (Chart 1, L) to host three amino acids, glycine, aspartic acid, and lysine, is investigated. The stability constants

Keywords: Molecular recognition; Amino acid complexes; Macrocyclic complexes.
☆Supplementary data associated with this article can be found, in the online version, at doi:10.1016/S0968-0896(03)00806-X
* Corresponding author. Tel.: +86-25359-3485; fax: +86-2533-14502; e-mail: chem1121@netra.nju.edu.cn

0968-0896/$ - see front matter © 2003 Elsevier Ltd. All rights reserved.
doi:10.1016/j.bmc.2003.11.020

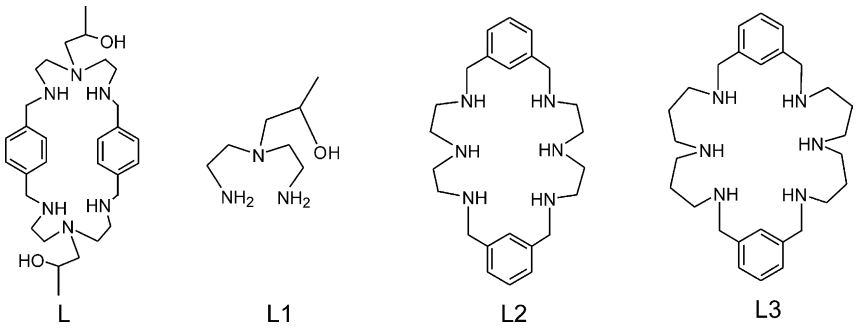

Chart 1.

for the binary complexes are reported and used to prepare distribution diagrams.

2. Experimental

2.1. Materials and instrument

C, H and N analysis were made on a Perkin–Elmer 240C elemental analyzer. ^{13}C NMR spectroscopic measurements were performed on a Brucker DRX-500 NMR spectrometer. 2-[Bis(2-aminoethyl)amino]-2-propanol (Chart 1, L1) was prepared as described in the previous literature.[12] The other reagents used throughout the experiments were of analytical grade from commercial sources and were used without any further purification.

2.2. Synthesis

The new macrocycle bearing 2-hydroxypropyl pendant, 6,19-bis(2-hydroxypropyl)-3,6,9,16,19,22-hexaaza-tricyclo - [22.2.2.2^{11,14}]triaconta - 11,13,24,26,27,29 - hexaene (L), was synthesized by the $NaBH_4$ reduction of the corresponding Schiff base obtained from the [2 + 2] condensation between 2-[bis(2-aminoethyl)amino]-2-propanol and terephthaladehyde similar to the reported procedure.[13] A solution of 98% terephthaladehyde (0.9973 g, 7.44 mmol) in MeCN (100 mL) was added dropwise to a solution of 2-[bis(2-aminoethyl)amino]-2-propanol (1.1978 g, 7.44 mmol) in MeCN (100 mL) at 0 °C under magnetic stirring over a period of 6 h. A white precipitate was produced after the reaction mixture was stirred for another 12 h at 0 °C. The solid products were filtered off and washed with ether, and then stored in a vacuum desiccator over silica gel. The ^{13}C NMR spectrum of the product in CD_3OD showed peaks at $\delta = 18.5$, 18.3 (CH_3), 162.9, 162.8 (CH=N), 136.8 and 127.5 (phenyl), 57.4, 57.1 and 64.6, 63.6 (NCH_2CH_2N), 53.6, 52.9 and 60.5, 59.9 ($NCH_2CH(CH_3)O$). This implies that the Schiff base has two (*cis*-, *syn*-) isomers in solution. The Schiff base (2.016 g, 4 mmol) was dissolved in absolute ethanol (100 mL) at 40 °C and sodium borohydride (0.5803 g, 15.39 mmol) was added gradually over a period of 4 h with constant stirring. After the addition of $NaBH_4$ was completed, the reaction solution stirred for another 12 h and then cooled to room temperature. The reaction mixture evaporated to dryness under reduced pressure. H_2O (3 mL) and acetone (3 mL) were added to the mixture to decompose the excess $NaBH_4$. After removing the solvent under reduced pressure, H_2O (5 mL) and CH_2Cl_2 (100 mL) were added sequentially to extract the product. Colorless viscous oil (L) was obtained when the organic phase was evaporated under reduced pressure to dryness. The ^{13}C NMR spectrum in D_2O gave peaks at $\delta = 45.5$ (CH_2 attached to phenyl), 136.7 and 128.4 (phenyl), 52.4 and 65.1 (NCH_2CH_2N), 51.5 and 61.3 ($NCH_2CH(CH_3)O$), 19.8 (CH_3). The two isomers of macrocyclic ligand can not be distinguished owing to rapid interchange of the two conformations in solution.[14] The ^{13}C NMR spectrum for the Schiff base and its hydrogenation products are shown in Figure S1 (see supplementary data). Several hours after the addition of 48% HBr (5 mL) to the product at 273 K, white microcrystals (L·6HBr) appeared in a yield of 2.7926 g (71%), and the synthetic path of L is shown in Scheme 1. Anal. calcd for $C_{30}H_{50}N_6O_2 \cdot 6HBr$ (1012.2): C, 35.56; H, 5.53; N, 8.30. Found: C, 35.55; H, 5.53; N, 8.21.

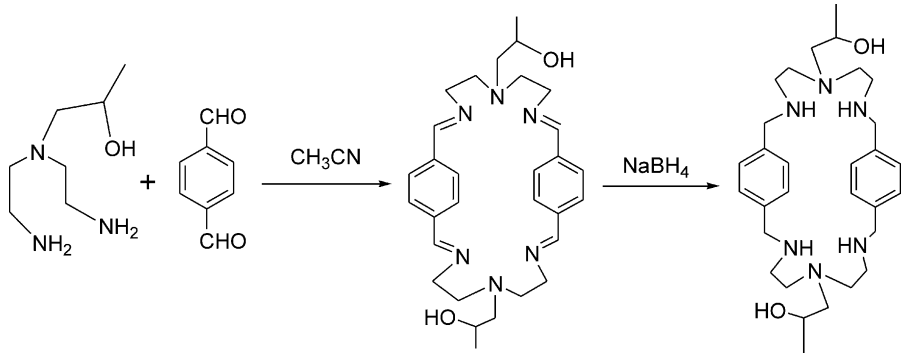

Scheme 1.

2.3. X-ray structure determinations

A colorless block single crystal for X-ray analysis was obtained by slow evaporation of a H_2O/MeOH solution of L·6HBr and $KClO_4$ in a 1:6 ratio for two days at ambient temperature. The data was collected on an Enraf-Nonius CAD-4 four-circle diffractometer by ω scan techniques using graphite-monochromated Mo-Kα radiation ($\lambda = 0.71073$ Å) at room temperature. The structure was solved by direct methods and refined on F^2 using the SHELXTL suite of program.[15] Hydrogen atoms were induced in calculated positions and treated as riding atoms using SHELXL-97 default parameters. Except the oxygen atoms of the water molecule and the disordered perchlorate anion, other non-H atoms were refined anisotropically. The crystallographic data are summarized in Table 1.

Crystallographic data for the structural analysis have been deposited with the Cambridge Crystallographic Data Center, CCDC reference number 210143. Copies of the data are available from http://www.ccdc.cam.ac.uk/prods/encifer/, quoting the deposition number.

2.4. Potentiometric equilibrium measurements

Potentiometric measurements of the protonation constants of the hexaaza macrocyclic ligand L and the stability constants of the binary complexes of the amino acids with the macrocycle were carried out with an Orion microprocessor ionalyzer-901 fitted with an Orion 91-04 glass combination pH electrode at 25 ± 0.1 °C. All aqueous solutions were prepared with distilled water, and the solutions were carefully protected from air by a stream of humidified nitrogen gas. Titrations were carried out in a temperature-regulated cell. The systems were calibrated with dilute standard acid and alkali solution. 1.0 M $NaNO_3$ was employed as supporting electrolyte to maintain the ionic strength $I = 0.10$ M. The value of $\log K_w$ for the systems is defined in terms of $\log([H^+][OH^-])$, was found to be -13.79 at the giving ionic strength and was maintained fixed during refinements. Stability constants and species distribution diagrams were calculated using the programs BEST and SPE, respectively.[16] All titrations contained approximately 1.0 mM macrocyclic ligand and appropriate ratios of other constituents. The protonation constants of the three amino acids used in the calculations were re-determined experimentally under the conditions employed here. All mixed systems titrations contained at least 90 points of data between pH 2.0 and 11.2. All data represent the average of at least two independent titration experiments.

Table 1. Summary of crystal data, data collection and refinement for $H_4L·Br_2·(ClO_4)_2·2H_2O$

Empirical formula	$C_{30}H_{58}Br_2Cl_2N_6O_{12}$
Formula weight	925.54
λ (Å)	0.71073
Crystal system	Monoclinic
Space group	$P2(1)/n$
a (Å)	10.757(2)
b (Å)	14.214(3)
c (Å)	13.746(3)
β (°)	101.40(3)
V (Å^3)	2060.3(7)
Z	2
ρ (g cm^{-1})	1.492
Measured reflections	3818
Unique reflections ($R_{int} = 0.0746$)	3617
Observed reflections [$I > 2\sigma(I)$]	1429
μ (mm^{-1})	2.159
Goodness-of-fit on F^2	1.005
$R1$, $wR2$ [$I > 2\sigma(I)$]	0.0695, 0.1538
Largest difference peak/hole (e Å^{-3})	0.876, −0.551

3. Results and discussion

3.1. Structure description of $H_4L·Br_2·(ClO_4)_2·2H_2O$

The perspective view of $H_4L·Br_2·(ClO_4)_2·2H_2O$ is shown in Figure 1. L was isolated as a mesomer, and the configuration of the chiral side chain of L is represented in Figure 1. Bond distances and angles and selected hydrogen-bonding data are listed in Tables 2 and 3, respectively. The compound crystallizes in the monoclinic system with the symmetry of space group $P2(1)/n$ and consists of a cation $[H_4L]^{4+}$, two bromide ions and two perchlorate anions, together with two crystalline water molecules. Chair conformation is adopted by the macrocycle with the crystallographic inversion center locating in the macrocyclic cavity. The four secondary nitrogen atoms are coplanar, while the nitrogen atoms of two tertiary amines deviate 0.62 Å from the plane, one up and one down. The benzene rings tilt at an angle of 70.3° to the former least-squared plane and keep parallel to each other with a distance of 8.49 Å. The two hydroxypropyl pendants appear at two different sides of the macrocycle plane and the distance between the two oxygen atoms of the hydroxypropyl pendants is 13.05 Å. The macrocyclic cavity may be described as an approximate ellipsoid with the major axis being the C15 to C15A distance of 12.24 Å and the minor axis being the N2 to N2A distance of 4.77 Å. The nitrogen atoms in the macrocycle are protonated except the tertiary ones, indicating that the tertiary amines are of weak bascity. The two bromide counterions are bound to the protonated amines through hydrogen bonds and encapsulated in the cavity formed by the macrocycle and the two hydroxypropyl arms. The Br1 atom forms

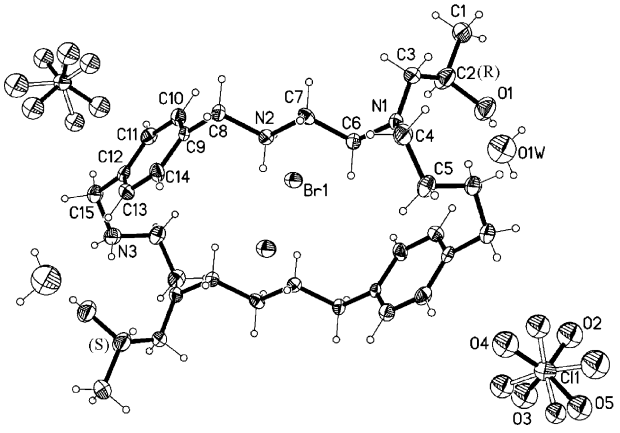

Figure 1. An ORTEP drawing of $H_4L·Br_2·(ClO_4)_2·2H_2O$.

two hydrogen bonds separately with N2 of two adjacent macrocyclic rings [N2...Br1 3.351(6) Å; N2...Br1^{i}, 3.290(6) Å], and simultaneously forms a hydrogen bond with the adjacent N3 atom [N3Br1^{v}, 3.373(8) Å] and O1W [O1W...Br1^{ii}, 3.184(10) Å], while O1W is connected with O1 through the hydrogen bond O1...O1W, 2.713(12) Å. The hydrogen bonds result in the formation of a two-dimensional layer onto *bc* plane as shown in Fig. 2. In addition, the π–π stacking interaction between the adjacent benzene rings of the two-dimensional layer structure with the nearest distance of 3.79 Å connect the 2-D layers to form an infinite three-dimensional network along the *a* axis.

It is of interest to compare the present structure with that of the unsubstituted macrocycles L2 and L3. In the crystal structure, the nitrogen atoms in the L are protonated except the tertiary nitrogen atoms, while all six nitrogen atoms are protonated in the L2 and L3.[4,17] The chair conformation of the macrocycle in this case is similar to that found in the crystal structure of L2 and L3. The macrocyclic cavity of L is similar to that of L2, and can be described as an approximate ellipsoid, but different from L3 in which the phenyl rings were nearly perpendicular to that plane which contains the rest of the aliphatic carbons and the six nitrogen atoms. The major axis (12.24 Å) of L is similar to that of L3 (12.89 Å), but longer than that of L2 (9.48 Å). The minor axis (4.77 Å) of L is longer than that of L3 (2.68 Å), but shorter than that of L2 (6.35 Å). Therefore, the presence of hydroxypropyl pendants makes the cavity size of L vary to a high degree with respect to the unsubstituted macrocycles.

Table 2. Bond length (Å) and angles (°) for $H_4L{\cdot}Br_2{\cdot}(ClO_4)_2{\cdot}2H_2O$

O(1)–C(2)	1.452(11)	N(2)–C(7)	1.493(9)
N(1)–C(6)	1.429(9)	N(2)–C(8)	1.504(8)
N(1)–C(3)	1.438(11)	N(3)–C(15)	1.488(10)
N(1)–C(4)	1.448(11)	N(3)–C(5)#1	1.488(11)
C(1)–C(2)	1.484(13)	C(9)–C(14)	1.383(11)
C(2)–C(3)	1.452(13)	C(10)–C(11)	1.388(11)
C(4)–C(5)	1.499(11)	C(11)–C(12)	1.383(11)
C(6)–C(7)	1.529(10)	C(12)–C(13)	1.356(11)
C(8)–C(9)	1.473(10)	C(12)–C(15)	1.480(11)
C(9)–C(10)	1.362(10)	C(13)–C(14)	1.389(12)
C(6)–N(1)–C(3)	116.9(8)	C(9)–C(8)–N(2)	109.9(6)
C(6)–N(1)–C(4)	115.1(7)	C(10)–C(9)–C(14)	116.2(9)
C(3)–N(1)–C(4)	119.0(8)	C(10)–C(9)–C(8)	122.7(8)
C(7)–N(2)–C(8)	113.9(6)	C(14)–C(9)–C(8)	121.2(8)
C(15)–N(3)–C(5)#1	115.9(7)	C(9)–C(10)–C(11)	122.8(9)
O(1)–C(2)–C(3)	108.3(9)	C(12)–C(11)–C(10)	119.5(8)
O(1)–C(2)–C(1)	110.9(9)	C(13)–C(12)–C(11)	119.2(9)
C(3)–C(2)–C(1)	115.2(9)	C(13)–C(12)–C(15)	120.6(9)
N(1)–C(3)–C(2)	114.4(9)	C(11)–C(12)–C(15)	120.2(9)
N(1)–C(4)–C(5)	110.1(7)	C(12)–C(13)–C(14)	120.0(9)
N(3)#1–C(5)–C(4)	108.4(8)	C(9)–C(14)–C(13)	122.3(9)
N(1)–C(6)–C(7)	113.2(7)	C(12)–C(15)–N(3)	113.3(7)
N(2)–C(7)–C(6)	110.1(6)		

Symmetry transformations used to generate equivalent atoms: #1−*x*−1, −*y*+2, −*z*+1.

Table 3. Selected hydrogen-bonding geometry (Å, °) for $H_4L{\cdot}Br_2{\cdot}(ClO_4)_2{\cdot}2H_2O$

D-H···A	D-H	H···A	D···A	∠D-H···A
O1-H1···O1W	0.82	1.90	2.713(12)	169
O1W-H1WA···Br1^{i}	0.96	2.28	3.184(10)	157
N2-H2B···Br1^{ii}	0.90	2.41	3.290(6)	165
N2-H2C···Br1	0.90	2.58	3.351(6)	144
N3-H3-D···Br1^{iii}	0.90	2.62	3.373(8)	142

Symmetry codes: (i) *x*+1/2, −*y*+5/2, *z*+1/2; (ii) −*x*-1, -*y*+2, −*z*+1; (iii) *x*-1/2, −*y*+5/2, *z*-1/2.

3.2. Protonation constants and stability constants of amino acids and L

The protonation constants of the three amino acids were re-evaluate at the experimental conditions used in this work. Their values and comparisons to literature values[18] are listed in Table S1 (see supplementary material). The difference between the constant values determined in the present work and those determined by others is minor.

In the absence of added substrate, a typical titration curve of 1.0 mM L with 6 equimolar HCl by 0.1 M NaOH solution at 25 °C is shown in Fig. 3. There is an inflection point at $a = 2.0$ (where a = number of moles of added base per mol ligand) observed in the titration curve. It indicates that the two tertiary nitrogen atoms are of very low basicity and release their protons easily

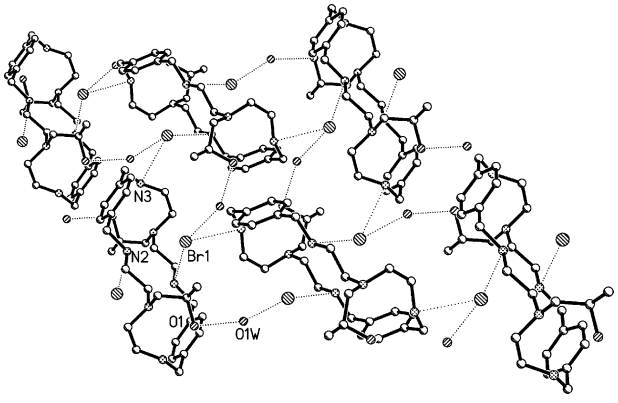

Figure 2. A perspective view of the two-dimensional network onto *bc* plane. H atoms and perchlorate have been omitted for clarity.

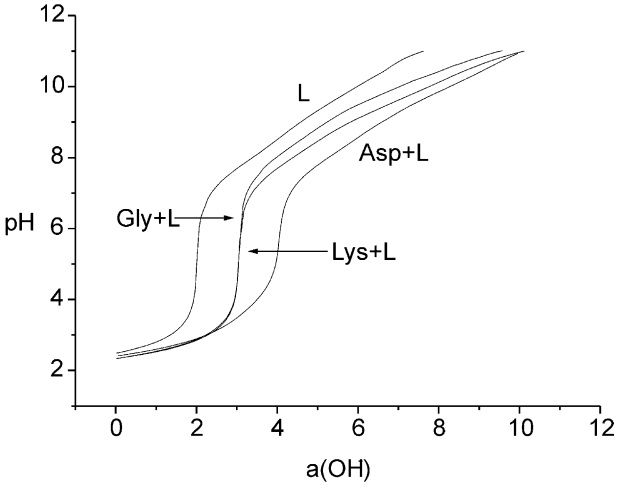

Figure 3. Typical titration curve at 25 °C and $I = 0.1$ M ($NaNO_3$).

into aqueous solution at low pH. The buffer region occurring at higher pH corresponds to the neutralization of the remaining four ammonium groups of the ligand in sequential overlapping steps. The titration data were analyzed for eqs 1–6. The protonation constants K_1–K_6 (α_{H+} is the activity of H^+) are defined as follows:

$$L + H^+ \rightleftharpoons HL^+ \quad K_1 = [HL^+]/[L]\,\alpha_{H+} \tag{1}$$

$$HL^+ + H^+ \rightleftharpoons H_2L^{2+} \quad K_2 = [H_2L^{2+}]/[HL^+]\alpha_{H+} \tag{2}$$

$$H_2L^{2+} + H^+ \rightleftharpoons H_3L^{3+} \quad K_3 = [H_3L^{3+}]/[H_2L^{2+}]\alpha_{H+} \tag{3}$$

$$H_3L^{3+} + H^+ \rightleftharpoons H_4L^{4+} \quad K_4 = [H_4L^{4+}]/[H_3L^{3+}]\alpha_{H+} \tag{4}$$

$$H_4L^{4+} + H^+ \rightleftharpoons H_5L^{5+} \quad K_5 = [H_5L^{5+}]/[H_4L^{4+}]\alpha_{H+} \tag{5}$$

$$H_5L^{5+} + H^+ \rightleftharpoons H_6L^{6+} \quad K_6 = [H_6L^{6+}]/[H_5L^{5+}]\alpha_{H+} \tag{6}$$

Logarithms of the protonation constants $\log K_1$–$\log K_6$ are 9.47, 9.25, 7.95, 7.44, 2.14, 0.55, respectively ($\sigma_{fit} = 0.013$). The species distribution for the protonated L system is displayed in Figure. 4, which shows H_4L^{4+} to be the major species from pH 3 to pH 6. It is seen that the fifth and sixth protonations constants are very small, which indicates the remaining two amine groups have low basicity. Considering that an efficient minimization of electrostatic repulsion between positive charges in the tetraprotonated species is possible through the localization of the four acidic protons in alternating position, the much lower fifth and sixth protonation constants are due to the fact that charge separation is no longer maximized.[8,19]

The much lower $\log K_5$ (2.14) and $\log K_6$ (0.55) of L than those of L2(3.79, 3.27) and L3 (7.20, 6.59)[4,17] may be caused by the addition of two hydroxypropyl which

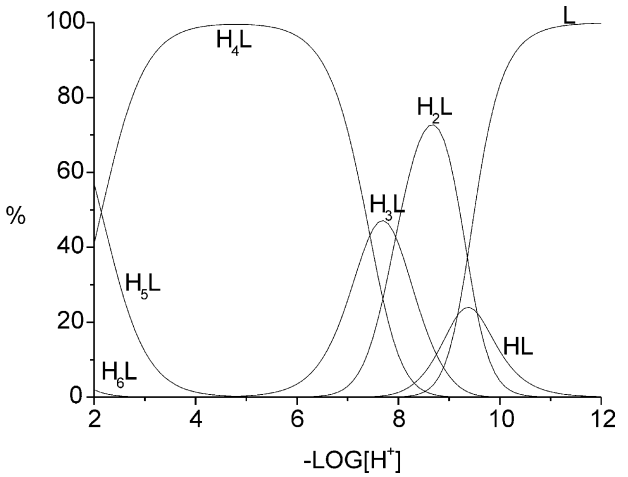

Figure 4. Species distribution graph as a function of pH for the 1 mM L system at 25 °C and $I = 0.1$ M ($NaNO_3$).

makes the tertiary amines are of weak bascity, and this is in accordance with the result of structure analysis. The other protonation constants of L (9.47, 9.25, 7.95, 7.44) are similar to those of L2 (9.51, 8.77, 7.97, 7.09), but all lower than those of L3 (10.33, 9.62, 8.57, 7.79). This difference is due to the fact that L3 contains one more methylene unit separating each two amino groups, helping to separate the positive charges when the corresponding amino groups are protonated.[17]

Potentiometric titration curve for a solution containing 1.0 mM glycine, 1.0 mM L and 7.0 mM HCl is shown in Figure 3. The titration curve of the system reveals an inflection at $a = 3$ (see Fig. 3); the first buffer region corresponding to the protonation of the two tertiary nitrogen atoms in the macrocycle and the carboxylate in glycine, which easily release their protons into aqueous solution at low pH. The equilibrium constants calculated for the binding of glycine to the protonated forms of L are listed in Table 4 ($\sigma_{fit} = 0.024$) and Figure 5(a) is the species distribution curves for a mixture of glycine and L in a 1:1 ratio. As shown in Figure 5(a), there are five species of protonated ligand-glycine are formed between pH 2.0–10.7. The binary species $GlyLH_5^{5+}$ is the major component from pH 3.5 to pH 7.0, and the abundance of it is about 30%.

Because of a weak complexation ability of monoprotonated L toward Gly, the abundance of the species $GlyLH^+$ is very small in the system, and the same case

Table 4. Stability constants for the L-glycine, L-aspartic acid, and L-lysine system ($I = 0.10$ ($NaNO_3$), 25.0 °C; Gly represents glycinate, Asp represents aspartate, Lys represents lysinate, H represents H^+)

Log K					
Gly		Asp		Lys	
		[AspLH]/[LH][Asp]	5.24		
[GlyLH$_2$]/[LH$_2$][Gly]	5.35	[AspLH$_2$]/[LH$_2$][Asp]	6.09	[LysLH$_2$]/[LH][LysH]	3.08
[GlyLH$_3$]/[LH$_3$] [Gly]	5.56	[AspLH$_3$]/[LH$_3$][Asp]	6.47	[LysLH$_3$]/[LH$_2$] [LysH]	3.83
[GlyLH$_4$]/[LH$_4$] [Gly]	6.33	[AspLH$_4$]/[LH$_4$][Asp]	7.06	[LysLH$_4$]/[LH$_4$] [LysH]	4.52
[GlyLH$_5$]/[LH$_5$] [Gly]	6.91	[AspLH$_5$]/[LH$_5$][Asp]	7.95	[LysLH$_5$]/[LH$_4$] [LysH]	5.03
[GlyLH$_6$]/[LH$_6$] [Gly]	7.60	[AspLH$_6$]/[LH$_6$][Asp]	8.53	[LysLH$_6$]/[LH$_5$] [LysH]	5.25
		[AspLH$_7$]/[LH$_6$][AspH]	5.32		

is also observed in lysine-L system. The macrocycle would be protonated when the pH value of solution decreased, and the positively charged macrocycle can bind the negative carboxylic group in glycine through hydrogen bond, which results in the content of $GlyLH_2^{2+}$ higher than $GlyLH^+$. As the positive charge of the ligand increased further, the hydrogen bond and coulombic attraction between glycine and L are increased also, and this is in accordance with the equilibrium constants lists in Table 4. Further protonation of the hepta-protonated binary species may not be possible because the positively charged diprotonated glycine molecules would not be attracted to the positively charged macrocyclic ligand.

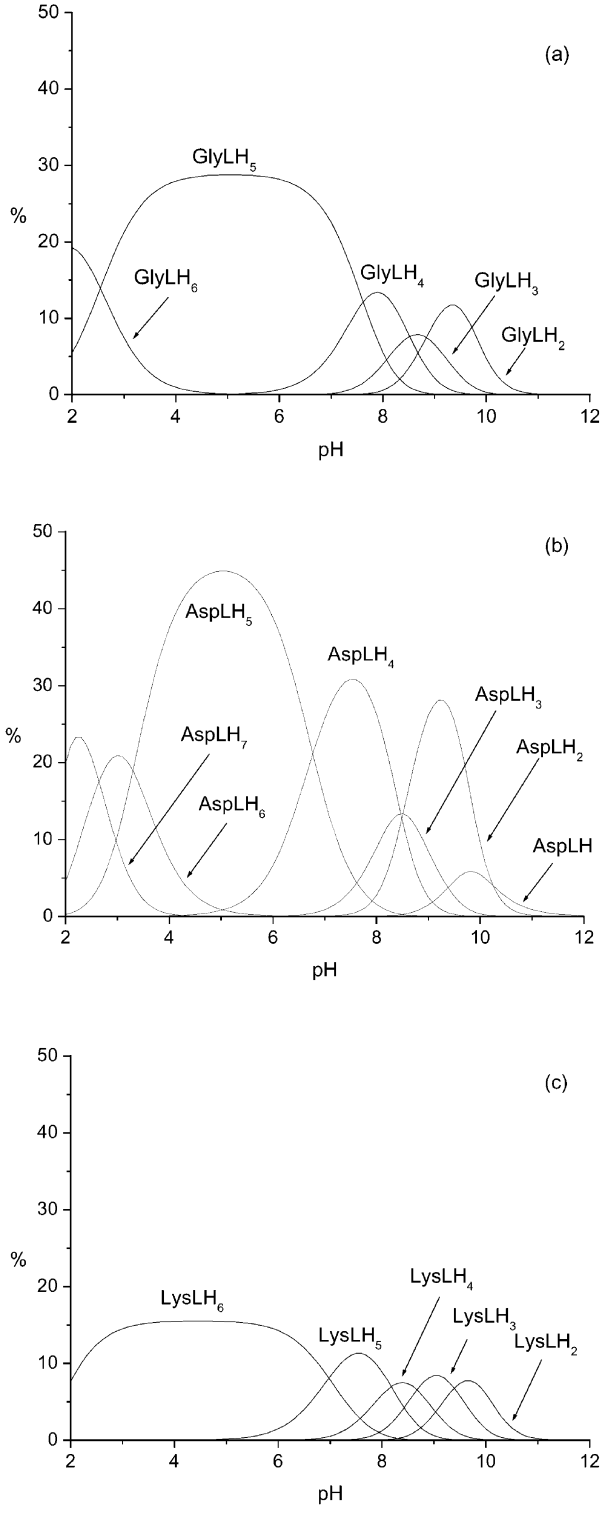

Figure 5. Differences in molecular recognition by L for the amino acids: (a) glycine; (b) aspartic acid; (c) lysine. In each case the total concentration of each component is 1.0 mmol at 25.0 C and $I = 0.1$ M ($NaNO_3$). Gly = glycinate, Asp = aspartate, Lys = lysinate.

The strongest binding mode of glycine and L in solution probably involves the negative carboxylic oxygens and amino nitrogen of glycine interacting with amino nitrogens of ligand through hydrogen bonding, and the suggested binding mode is shown in Chart 2. This is tally with the fact that $GlyLH_5^{5+}$ is the predominant species through a wild pH range.

Figure 5(b) displays the species distribution as a function of pH at a total aspartic acid concentration of 1.0 mM and total L concentration of 1.0 mM with 7 equimolar HCl at 25 °C. Table 4 ($\sigma_{fit} = 0.033$) gives the binding constants for the interaction of L and aspartic acid. In comparison with the glycine-L binary systems, L is shown to recognize aspartic acid with greater affinity and seven different protonated binary species are seen to form. The titration curve of the system (Fig. 3) shows that there is an inflection point at $a = 4.0$, which indicates that the two protonated tertiary nitrogen atoms in the macrocycle and the two carboxylic acid group in aspartic acid easily release their protons into aqueous solution at low pH.

Complex species have been detected that involve the association of the aspartate with the mono- through hexa-protonated L. The log values of the stepwise association constants for these species increase as the degree of protonation increases. This may be due to the increased degree of protonation for the macrocycle which leads to a greater coulombic attraction and the increasing hydrogen bonding interaction between the ligand and aspartic acid. A further protonated species $AspLH_7^{7+}$ is also detected, and the only possible bonding mode for it is hydrogen bonding between the most acidic carboxylate groups and protonated amino groups on the macrocyclic ligand.[2] The log association constant for this species is smaller than the previous member of the series, maybe because the hexa-protonated ligand is unstable in solution. This is consistent with the species distribution graph for the macrocycle ligand which shows H_6L^{6+} can only exist as a minor species around

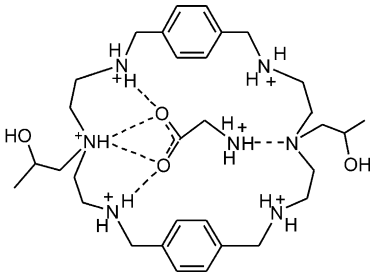

Chart 2. Suggested binding pattern of glycine in penta-protonated binary species $GlyLH_5^{5+}$.

pH 2.0 (Fig. 4). The species $AspLH_5^{5+}$ reach a maximum around pH 5.0 with an abundance of 45%, which is higher than the other two amino acids. The protonation results show that the additional carboxylic acid group on the aspartic acid can increase the negative charge on the species throughout most of the pH range, which leads to the existence of highly protonated binary species and the greater affinity for recognition in aqueous solution.

Figure 5 (c) is the distribution species graph of 1.0 mM lysine and 1.0mM L with 8 equimolar HCl by 0.1 M NaOH solution at 25 °C. As shown in Figure 5 (c), that lysine forms five binary species, the hexa-protonated binary species exist as a single principal species over a wide range from pH 2–pH 6.5 in aqueous solution with an abundance of 15%. The binding constants for the binary species formed from lysine and protonated L are listed in Table 4 ($\sigma_{fit} = 0.021$). The cations LH^+ through LH_5^{5+} form binary complexes with $LysH^+$, the association constants increasing as the degree of protonation of the macrocycle increases, and the hexa-protonated binary species exists as a predominant species from low pH up to pH 6.5. Between pH 3 and 6.5, the $GlyLH_5^{5+}$ is the major species in L-glycine system, while $LysLH_6^{6+}$ is predominant in L-lysine system. This maybe because lysine has one more amino group which can be protonated easily at low pH. Although lysine has an additional amino group, it can not form more binary species than glycine, and the binding affinity that L shows for glycine is larger than that for lysine. This may be because of weaker complexation of multicatronic L with monocatronic lysine than that with neutral glycine.

The results of potentiometric study show that the new macorcyle can recognize the above three kinds of amino acids selectively, and the order of increasing abundance of various binary species (of L-amino acid) was found to be lysine is about 15%, glycine is about 30% and aspartic acid is about 45%. The binary species of L and amino acids are formed mainly through electrostatic attractions and hydrogen bonding forces in these systems. But it is difficult to uniquely quantify the relative contributions of pure electrostatic attractions and hydrogen bonding forces in the carboxylate affinity for protonated amines since the ammonium groups by definition all possess a potentially bindable extra proton.

4. Conclusion

A new macrocyclic ligand with two hydroxypropyl pendants have been synthesized and characterized by potentiometric analysis. Form the potentiometric studies it is found that L is able to bind aspartic acid with the greatest affinity, while that the degree of complex formation of lysine with L is the smallest. The existence of highly protonated binary systems and the recognition with greater affinity for aspartic acid maybe because that the additional carboxylic acid group on the aspartic acid results in an increased negative charge on the species throughout most of the pH range. The binding affinity that L shows for glycine is larger than that for lysine, and it may be due to the weaker repulsion to the positive charge of glycine than that of lysine.

Acknowledgements

This work was supported by the National Nature Science Foundation of China

References and notes

1. Shangguan, G. Q.; Martell, A. E.; Zhang, Z. R.; Reibenspies, J. H. *Inorg. Chim. Acta* **2000**, *299*, 47.
2. Ross, E.; Motekaitis, R. J.; Martell, A. E. *Inorg. Chim. Acta* **1999**, *286*, 55.
3. Aguilar, J. A.; Clifford, T.; Danby, A.; Llinares, J. M.; Mason, S.; Garcia-Espana, E.; Bowman-Espana, K.; Bowman-James, K. *Supermol. Chem.* **2001**, *13*, 405.
4. Nation, D. A.; Reibenspies, J.; Martell, A. E. *Inorg. Chem.* **1996**, *35*, 4597.
5. Nation, D. A.; Lu, Q.; Martell, A. E. *Inorg. Chim. Acta* **1997**, *263*, 209.
6. Lu, Q.; Motekaitis, R. J.; Reibenspies, J. J.; Martell, A. E. *Inorg. Chem.* **1995**, *34*, 4958.
7. Anda, C.; Llobet, A.; Salvado, V.; Martell, A. E.; Motekaitis, R. J. *Inorg. Chem.* **2000**, *39*, 3000.
8. Gerasimchuk, O. A.; Mason, S.; Llinares, J. M.; Song, M.; Alcock, N. W.; Bowman-James, K. *Inorg. Chem.* **2000**, *39*, 1371.
9. Andrés, A.; Aragó, J.; Bencini, A.; Bianchi, A.; Domenech, A.; Fusi, V.; García-España, E.; Paoletti, P.; Ramírez, J. A. *Inorg. Chem.* **1993**, *32*, 3418.
10. (a) For selected recent reviews. See: A. E. Martell, In *Crown Compounds: Towards Future Applications*; S. R. Cooper, Ed.; VCH Publishers: New York, 1992; Chapter 7, p 99. (b) Mertes, M. P.; Mretes, K. B. *Acc. Chem. Res.* **1990**, *23*, 413. (c) Lzatt, R. M.; Pawlak, K.; Bradshaw, J. S.; Bruening, R. L. *Chem. Rev.* **1991**, *91*, 1721. (d) Dietrich, B. *Pure Appl. Chem.* **1993**, *65*, 1457. (e) Menger, F. M.; Catlin, K. K. *Angew. Chem., Int. Ed. Engl* **1995**, *34*, 2147.
11. Antonisse, M. M. G.; Reinhoudt, D. N. *Chem. Commun.* **1998**, 443.
12. Dow Chemical Co. Fr. 2112697, 1972-07-28. (From CA 78: 124002g)
13. Li, S.-A.; Xia, J.; Yang, D.-X.; Xu, Y.; Li, D.-F.; Wu, M.-F.; Tang, W.-X. *Inorg. Chem.* **2002**, *41*, 1807.
14. Li, S. A.; Li, D. F.; Yang, D. X.; Li, Y. Z.; Huang, J.; Yu, K. B.; Tang, W. X. *Chem. Commun.* **2003**, 880.
15. G. M. Sheldrick, SHELXTL ver. 5.10, Program for Crystal Structure Determinations, Siemens Industrial Automation Inc., Madison, MI, 1997.
16. Martell, A. E.; Motekaitis, R. J. *Determination and Use of Stability Constants*, 2nd ed.; VCH: New York, 1992.
17. Llobet, A.; Reibenspies, J.; Martell, A. E. *Inorg. Chem.* **1994**, *33*, 5946.
18. A. E. Martell, R. M. Smith, Critical Stability Constants Volume 5: First Supplement, New York, 1982.
19. Bencini, A.; Bianchi, A.; Garcia-España, E.; Micheloni, M.; Ramirez, J. A. *Coord. Chem. Rev.* **1999**, *188*, 97.